INTERNATIONAL JOURNAL OF PRECISION ENGINEERING AND MANUFACTURING Vol. 16, No. 2, pp. 361-366 FEBRUARY 2015 / 361
DOI: 10.1007/s12541-015-0047-8

Fabrication of Microchannels on Transparent PMMA Using CO_2 Laser (10.6 μm) for Microfluidic Applications: An Experimental Investigation

Shashi Prakash[1] and Subrata Kumar[1,#]

1 Department of Mechanical Engineering, Indian Institute of Technology Patna, Patna, 800013, India
Corresponding Author / E-mail: subrata@iitp.ac.in, TEL: +91-612-255-2039, FAX: +91-612-227-7383

KEYWORDS: Laser micromachining, CO_2 Laser, PMMA, Microfluidics

In this research work, microchannel fabrication on PMMA (Polymethyl-methacrylate) using a CO_2 laser has been investigated thoroughly. Microchannels have been created on PMMA of diverse aspect ratio. Due to Gaussian nature of beam, the channel cross-section also possesses the near Gaussian shape. The optical properties of PMMA have been investigated using Far-infrared spectroscopy and micro-hardness test has been carried out to verify the presence of softened zone adjacent to laser ablated microchannels. To investigate the effects of individual parameters on microchannel fabrication, 27 numbers of experiments have been performed using full factorial method. Mathematical modeling of each parameter has been performed using nonlinear regression analysis of each factor. The effect of each input parameter viz. laser power, scanning speed and number of pulses per linear inch has been discussed on each microchannel characteristics. Multi-objective optimization has been performed based on desirability function. The results of this work will be further useful in developing fundamental theoretical models for laser ablation of microchannels on PMMA.

Manuscript received: January 24, 2014 / Revised: August 20, 2014 / Accepted: October 22, 2014

1. Introduction

Microfluidics applications involving microchannels on different types of the materials are need of today. These microchannels based devices are mainly used in biological applications, chemical analysis and in many analytical and testing devices including DNA analysis, protein analysis and blood sample analysis.

Fabricating microchannels on conventional materials like soda-lime glasses, silicon and quartz require the use of photolithography procedures and wet chemical etching to make patterns on substrate material for microchannel configurations.[1] These procedures result in formation of significant burrs around the microchannels as well as the process becomes tedious, costly and time consuming. Apart, skilled labor is required to fabricate the microchannels.

Recently, PMMA (Polymethyl methacrylate) based microchannels have come up as a cost effective solution to many microfluidic devices. Transparent PMMA offers the advantage of low weight, high visibility and low cost solution which makes it more useful to use it as portable and cheap device. PMMA, due to its high transparency, can be used as a replacement of glass based microfluidic devices. It is predominantly used as drug delivery system material, implants and possesses high biocompatibility.[2,3]

Fabrication of microfluidic channels on PMMA has been done using standard lithography process[4] as well as hot embossing process,[5] femtosecond laser processing,[2] and excimer laser.[6] However, the standard lithography involves various steps in processing and its high associated cost. The femtosecond lasers are less common in modern industries because of its high cost and excimer laser involves sophisticated beam optics which is difficult to maintain in large production houses. Microchanneling by CO_2 laser processing is one step processing which involves minimum time consumption. Laser micro-processing has enabled the production of microfluidic systems with lowest cost per unit when compared to other contemporary methods. PMMA is highly transparent for visible light. At the same time, it acts as a perfect absorber in far-infrared zone as well as in ultraviolet region. Therefore, the UV lasers as well as CO_2 lasers having beam wavelengths outside the human visible range can only be applied in transparent PMMA processing.

Theoretical aspects of CO_2 laser ablation of PMMA has been studied by Klank et al[7] and Snakenborg et al..[8] Birkett[9] has studied the phenomenon of CO_2 laser cutting and drilling on PMMA. Laser microchanneling on black laden PMMA using Nd:YAG laser has been attempted by Prakash et al.[10] Only the transparent PMMA can be utilized in most of the microfluidic devices.

Microfluidic applications involve microchannels having wide range of dimensions. Some of the applications like particle separation devices require low aspect ratio microchannels[11] while many other require high aspect ratio. Theoretically, with the ideal optics, the minimum CO_2 laser beam diameter is given by $d_{min} = 1.22\lambda/NA \approx \lambda$ (Asibu Jr.),[12] where λ is wavelength of the laser beam i.e., 10.6 μm and NA is numerical aperture of the focusing lens. However, in actual, with the most advanced optics "HPDFO" (high power density focusing optics), the minimum beam diameter practically achieved is 38 μm.[13] Few authors have used masks and stencils to achieve features which are typically less than 50 μm.[14,15] With the proper control of input parameters like laser power, focal length and scanning speed, smaller features can also be created without the need of masks and stencils. However, in such cases, achieving higher channel depth might be difficult. Yuan & Das[16] have achieved width and depth as small as 44 and 22 μm. Zakariyah et al.[17] have also achieved the dimensions as small as 20 μm.

However there is significant lack of research in microchanneling process using CO_2 laser when detailed experimental point of view is concerned. Fabrication of high aspect ratio microchannels on PMMA have not been studied in much detail earlier. Especially the effects of process parameters on softened zone and the effect of number of pulses per linear inch (PPI) has not been discussed before. In this work, a detail study of experimental aspects of microchannel machined by a CO_2 laser combined with physical insight of cutting mechanism on PMMA has been presented. Study has been focused on fabricating microchannels of diverse aspect ratios. The developed mathematical model and optimization results cover a large range of microchannels with smaller as well as higher dimensions.

2. Determination of PMMA Properties

In order to determine the absorptivity of PMMA for CO_2 laser wavelength i.e., at 10.6 μm, far-infrared (FIR) spectroscopic analysis has been performed using Shimazdu IRAffinity-1 spectrophotometry. In this experiment cast acrylic (PMMA) of 3 mm thickness has been used. The transmissivity results are shown in Fig. 1. The transmissivity corresponding to 10.6 μm (943 cm^{-1}) has been found to be 0.31%. Therefore, it can be assumed that PMMA absorbs nearly 95% (Reflectivity = 4.67%) of CO_2 laser wavelength.

Other than optical properties, thermal properties of PMMA are quite common and readily available. PMMA starts to change its nature from solid to rubbery state at 115°C (glass transition temperature) which forms the softened zone.[16]

3. Experimental Details

In this research work, commercial CO_2 laser, (VLS 3.60, Universal Laser System Inc., USA), having maximum average power of 60 W has been used in fabricating microchannels on PMMA (Fig. 2). The detailed specification of laser system has been given in Table 1.

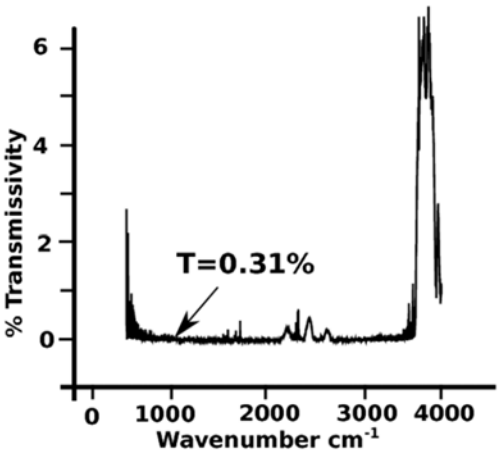

Fig. 1 Far-Infrared (FIR) spectroscopy result of transparent PMMA

Fig. 2 CO_2 laser system used in the experiment

Table 1 CO_2 Laser system specification

Class type	IV
Max. average power	60 W
wavelength	10.6 μm
Output beam shape	Gaussian
M^2 value	1.5
Mode of operation	RF excited pulse ON/OFF
Beam diameter at focus	237 μm

3.1 Laser input parameters and microchannel characteristics

For this CO_2 laser the basic input parameters, which affect the microchannel fabrication, are average power (P), scanning speed (U), and pulse per linear inch (PPI) (N).

The output characteristics for microchannel have been taken as top width of the microchannel, depth of the microchannel and laser softened zone at the top surface (Fig. 4). All three output characteristics have been measured using Olympus optical microscope STM-6.

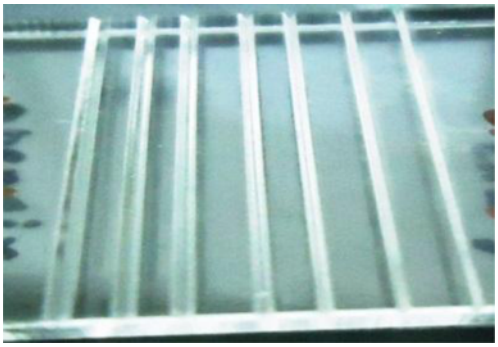

Fig. 3 Microchannels fabricated on PMMA workpiece

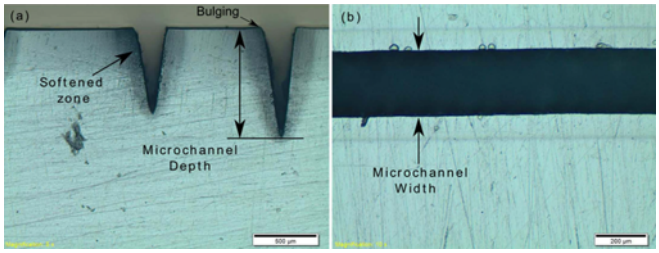

Fig. 4 (a) Cross-sectional view and (b) Top view of microchannel

Table 2 Factors and level considered for microchanneling

Input parameters	Designation	Level 1	Level 2	Level 3
Average Power (W)	P	2	3	4
Scanning speed (mm/sec)	U	5	7.5	10
PPI	N	500	700	900

3.2 Design of experiments

After conducting various pilot experiments to create a range of diverse aspect ratio microchannels, three levels of each input parameters have been selected.

In order to fully investigate the effect of each process parameter on output characteristics, total 27 (3^3) number of experiments have been performed. The design of experiment has been created using JMP software (SAS Inc., USA). The details of experimental runs and corresponding values of responses are given in Table 3.

For measuring the output parameters, the specimens have been prepared with fully polished sides. Microchannel width and softened zone width has been measured directly from the top view while the depth has been measured after carefully preparing the sides using polishing paper and ultrasonic cleaning (Fig. 4).

Laser softened zone, which is comparatively a new term has been verified by using Zwick /Roell Indentec micro-hardness tester. The hardness of the softened zone and outside surface has been measured at various locations. The applied load is 25 gf and Vickers hardness value has been found to be 22 HV outside the softened zone while the hardness inside softened zone is found to be 18 HV. Due to this reduction in hardness, the adjacent part has been termed as softened zone. The hardness values are found to be constant inside softened zone at various locations (Fig. 5). The formation of laser softened zone takes place due to conversion of adjacent material into rubber-like state when the temperature crosses the glass transition temperature of the material i.e., 115°C. The series of microchannels created on a PMMA sample has been shown in Fig. 3. The extent of softened zone fully depends on thermal conductivity of the material and is a volumetric phenomenon as evident in cross-sectional pictures. The softened zone width boundary lies within a boundary where the temperature during the processing lies between vaporization temperature and glass transition temperature.

Table 3 Design of experiments and responses

SI No.	Input parameters			Output parameters			Total transferred energy (mJ/mm)
	Power (W)	Scanning speed (mm/sec)	PPI	Width (μm)	Depth (μm)	Softened zone (μm)	
1	4	10	700	276.33	879.4	120.25	380
2	2	7.5	500	272.49	569.24	101.06	253.33
3	2	7.5	900	255.86	582.12	108.74	253.33
4	2	10	700	262.26	504.85	106.18	190
5	3	7.5	900	271.21	850	113.05	380
6	4	5	900	301.91	1553.19	153.63	760
7	3	5	700	295.52	1253.94	143.28	570
8	3	5	900	287.84	1233.79	140.12	570
9	4	7.5	700	290.4	1094.7	145.84	506.66
10	3	10	900	259.7	678.03	99.86	285
11	3	7.5	500	291.68	837.12	110.06	380
12	2	7.5	700	262.26	623.34	118.97	253.33
13	2	5	900	273.77	847.43	125.37	380
14	3	10	700	268.65	686.52	101.06	285
15	3	7.5	700	276.33	916.97	122.81	380
16	4	10	500	287.84	865.46	111.3	380
17	2	10	900	237.95	471.37	93.39	190
18	2	10	500	263.54	437.88	86.99	190
19	2	5	500	286.56	852.58	115.14	380
20	2	5	700	280.84	858.79	135.61	380
21	4	7.5	500	299.36	1066.37	122.81	506.66
22	4	7.5	900	276.33	1063.79	136.88	506.66
23	4	10	900	267.37	855.15	118.97	380
24	3	10	500	269.93	672.27	98.51	285
25	4	5	700	305.75	1561.2	156.07	760
26	3	5	500	303.19	1210.49	138.16	570
27	4	5	500	312.15	1542.88	150.96	760

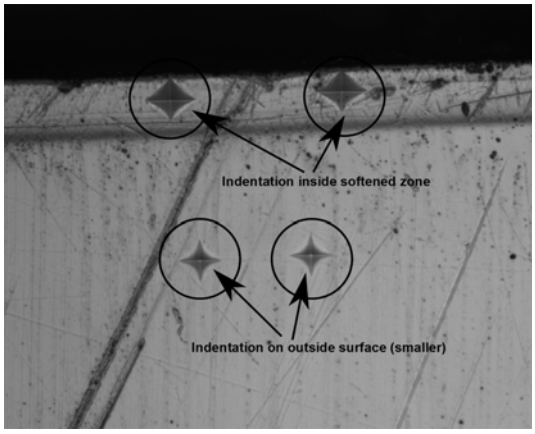

Fig. 5 Micro-hardness test at 25 gf load

The softened zone can be visualized in Fig. 4. Presence of bulging at the upper corners can also be realized in this figure. The bulging height normally ranges between 1~10 μm.

4. Interaction of CO_2 laser with PMMA

CO_2 laser ablation is purely thermal ablation in which material removal takes place purely due to melting and vaporization. PMMA strongly absorbs the CO_2 laser and vaporizes immediately as soon as the average laser power crosses certain threshold value. It can also be assumed that material removal process involves direct sublimation of solid PMMA into vapors without melting. This is one of the reasons that CO_2 laser ablation of PMMA does not involves redeposition of materials. Therefore the cut is almost clean with very little or no defects. However a little charring and burning effects are quite visible at the edges forming the buldging zone. The only undesirable effect is softened zone and bulging of the material at the adjacent surfaces. Under the incident laser beam the temperature of the surface immediately rises to its vaporization temperature and PMMA $(C_5O_2H_8)_n$ decomposes into monomer MMA (methyl methacrylate) units, carbon dioxides (CO_2), carbon monoxides (CO) and water $(H_2O)_{10}$. All the byproducts are perfectly volatile in nature and do not cause any further reaction on the PMMA substrate, leaving behind a clean structure. Due to low thermal conductivity of the PMMA the heat gets accumulated inside the adjacent layer and therefore can be attributed for the formation of bulges and softened zone. The formation of bulges specially takes place at locations which are subjected to temperature ranges in between melting temperature and phase change temperature.

5. Effects of PROCESS PARAMETERS

5.1 Pulse overlapping and total transmitted energy

PPI is the primary cause of pulse overlapping. Pulse overlap can be defined by using following Eq. 1:[18]

$$pulse\ overlap = (1 - U/(f \cdot d)) \times 100\% \quad (1)$$

Where f is pulse repetitive frequency (N×U) and d is the beam diameter. Pulse overlapping with corresponding PPI has been given in Table 4. Pulse overlapping affects the surface properties of the machined microchannel. Larger pulse overlapping produces smoother surface. Pulse overlapping also affects the microchannel dimensions, though less dominantly.

The total transmitted energy (mJ/mm) can be defined as amount of energy transferred to the material per unit length and can be calculated using Eq. (2).

$$\text{Total transmitted energy} = \text{absorptivity} \times (P/U)\ (\text{mJ/mm}) \quad (2)$$

Total transmitted energy has been calculated for each experiment as shown in Table 3. The total power of the beam gets divided into number of pulses. The largest transmitted energy of 760 mJ/mm takes place in experiment number 6, 25 and 27. Therefore, the largest microchannel dimensions occur in these experiments. Similarly lowest energy transfer (190 mJ/mm) takes place in experiment number 4, 17 and 18 leading to lowest microchannel dimensions. It should be noted that total transmitted energy is independent of PPI parameter. The difference in microchannel dimensions of same energy absorption can be attributed to pulse overlapping effect.

Table 4 PPIs and corresponding pulse overlap

PPI	Pulse overlap %
500	59.34
700	70.96
900	77.42

5.2 Effects of process parameters on responses

5.2.1 Microchannel width

The microchannel width (at the top) varies from 237 μm to 312 μm. As the average laser power increases the width of the microchannel also increases. Higher laser power results in energy transfer at a high rate to the specimen. At lower number of pulses per linear inch (PPI) i.e., at PPI=500 (60% pulse overlap), the average energy of the pulse increases when compared to higher PPI as the average energy has to be distributed in lesser number of pulses. Therefore the maximum width occurs at highest power combined with lowest speed and lower PPI (experiment no. 27). Also as the scanning speed increases the width of the microchannel decreases (Fig. 6(a)). This is very much obvious since increasing the velocity results in lower energy transfer per unit length to the material. Also, since the pulse overlap gets reduced; the reduction in energy accumulation per unit area takes place resulting in lower channel width.

5.2.2 Microchannel depth

The depth of microchannel varies from 437 μm to 1561 μm with aspect ratios ranging from 1.5 to as high as 5. With increase in average laser power, the depth of the microchannels increases as larger power is directly responsible for transfer of more energy resulting in more heat generation and larger material removal. Depth of the microchannel gets reduced with increase in scanning speed because of the lower amount of energy transfer per unit length. The rate of depth reduction directly depends upon scanning speed as evident by Fig. 6(b). As the PPI increases, the average energy of the pulse decreases. However at the same time high PPI causes more pulse overlapping which also affects the process. By observing the data carefully it can be deduced that most effective depth takes place at 700 PPI (71% overlapping). This phenomenon can be explained as a combined effect of pulse overlap and average energy of the pulses. At high PPI i.e., at 900 PPI the average energy of laser pulses are less effective. At 700 PPI the combinatory effect of pulse overlap as well as average pulse energy is found to be more effective than high pulse energy but less pulse overlap at 500 PPI.

5.2.3 Softened zone

The extent of softened zone width varies from 86 μm to 156 μm. The main effect plots for softened zone have been given in Fig. 6(c). The softened zone increases with increase in power at all PPIs. As the

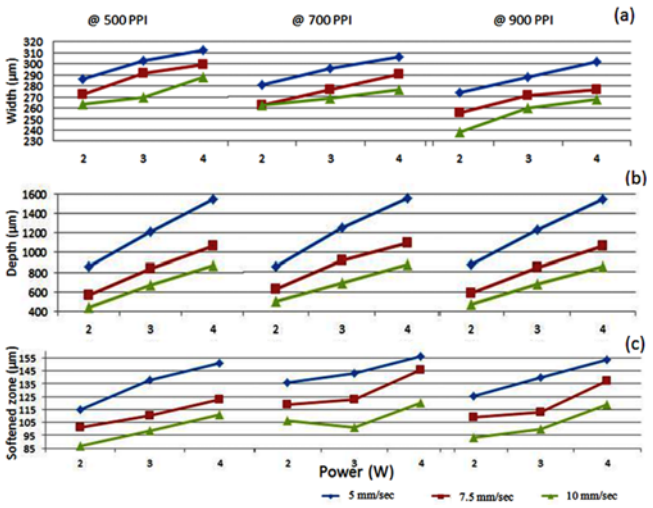

Fig. 6 Main effect plots for (a) microchannel width, (b) microchannel depth, (c) Softened zone

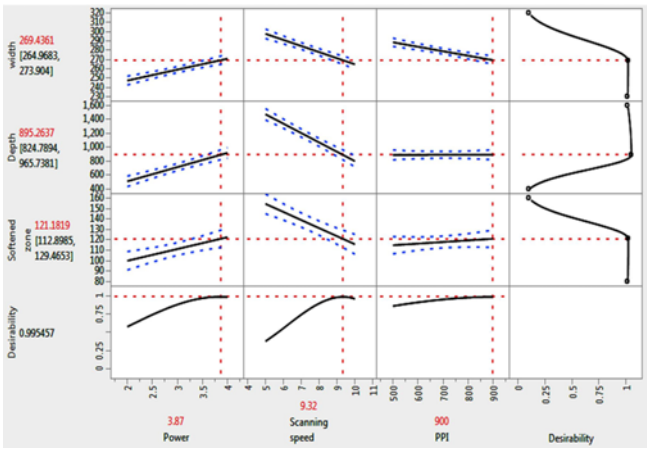

Fig. 7 Multi-objective optimization results

laser power increases, the more energy is available to conduct in surrounding zone and therefore the extent of softened zone increases. With increase in scanning speed the width of the softened zone decreases as lesser amount of energy is available to conduct in adjacent layers. The highest softened zone is associated with 700 PPI followed by 900 PPI and 500 PPI. At 700 PPI the combinatory effect of average pulse energy and effective overlapping of pulses takes place. However, at 900 PPI, the numbers of effective pulses are more with lesser energy. The large number of pulses causes an immediate increase in softened zone. At 500 PPI, the numbers of effective pulses are less but the concentrated energy is larger, therefore more energy is allowed to get transfer in direction of beam movement rather than in surrounding layers, therefore a decrease in softened zone width takes place.

6. Process Modeling and Optimization

Simple non-linear regression predictive models have also been developed for all the three responses. P, U & N denote average laser power, scanning speed and PPI respectively in Eqs. (3), (4) and (5). In the Eq. (3), it can be observed that power term has the highest coefficient and therefore predominantly affects the microchannel width followed by scanning speed. PPI has relatively insignificant effect on the width of the microchannel. In Eq. (4) the coefficient for power term is highest and therefore has the most significant effect on depth followed by scanning speed and PPI. In the regression model for softened zone (Eq. (5)), again power is the most significant term and should be varied carefully to obtain minimum thickness of softened zone. It should be noted that in prediction modeling of softened zone, only the interaction term of power and speed are significant while all other interaction terms are insignificant and therefore have been ignored.

$$\text{Width} = 314.59+12.328\times P-5.6435\times U-0.043\times N-0.361667 \times P\times U+0.0005\times P\times N-0.002\times U\times N \quad (3)$$

$$\text{Depth} = 915.75+263.03\times P-108.075\times U+0.0223\times N-0.3041 \times P\times U-0.01825\times P\times N+0.00008\times U\times N \quad (4)$$

$$\text{Softened zone} = 126.69+12.51\times P-7.15\times U +0.015\times N-0.686\times P\times U \quad (5)$$

For fabricating microchannels of high aspect ratio, the responses have been optimized as:

1. Width should be minimized
2. Depth should be maximized
3. Softened zone should be minimized

Therefore, the process has been optimized using desirability based multi-response optimization process. A typical desirability function for multi-objective optimization is based on geometric means of all transformed responses d_i (average of natural logs of desirabilities).[19]

For k responses,

$$D^* = {}^k(d_1\times d_2\times d_3\ldots d_k) \quad (6)$$

Where D^* is transform desirability. The actual overall desirability can be computed as,

$$D = \ln(D^*) = 1/k\ [\ln(d_1)+\ln(d_2)+\ldots\ln(d_k)] \quad (7)$$

All the responses have been given equal weight i.e., 0.333.

As the Fig. 7 depicts the optimized values of Power, scanning speed and PPI are 3.87 W, 9.32 mm/sec and 900 respectively at the desirability function value of 0.99 which is very close to 1. This further signifies that the optimization result is very much close to desirable result.

7. Conclusion

In this study, thorough investigation of laser induced microchannel characteristics i.e., microchannel width, microchannel depth and softened zone has been performed.

The spectroscopic results prove the utility of CO_2 laser in machining PMMA with very high efficiency. The CO_2 laser does not cause residual

stress or cracks as evident by optical micrographs during machining. The micro hardness test reveals the presence of softened zone due to transition of solid state PMMA into rubbery state PMMA, just adjacent to microchannels. The developed process models for individual parameters can be used directly in industrial purposes. Since PMMA is highly absorbing for CO_2 laser wavelength, even a slight change in laser power affects all three microchannel characteristics predominantly. In order to find out most favorable condition for machining, the multi-objective optimization has been carried out. To verify the optimization results, the confirmation experiment has been carried out. The presence of softened zone plays a vital role in fabricating microfluidic devices on PMMA since it leads to bulges and therefore must be minimized. The predicted models can readily be used to predict the microchannel dimensions for input parameters in this range. The optimized results can be used to obtain best quality microchannel in this range.

CO_2 laser microchanneling is a clean and effective process for fabricating microfluidic devices. However, in most of the microfluidic devices, surface qualities also play a very vital role. Most of the microfluidic devices need surface roughness to be lower than 1 μm. Many devices need the surface to be hydrophilic while some needs hydrophobic surfaces. The contact angle of the surfaces with different kind of fluids also has significant effect on practical utilization of these microchannels.

ACKNOWLEDGEMENT

Authors deeply acknowledge the financial support of Department of Science and Technology, Government of India for providing INSPIRE fellowship.

REFERENCES

1. Hong, T. F., Ju, W. J., Wu, M. C., Tai, C. H., Tsai, C. H., and Fu, L. M., "Rapid Prototyping of PMMA Microfluidic Chips Utilizing a CO_2 Laser," Microfluidics and Nanofluidics, Vol. 9, No. 6, pp. 1125-1133, 2010.
2. Fernández-Pradas, J., Florian, C., Caballero-Lucas, F., Morenza, J., and Serra, P., "Femtosecond Laser Ablation of Polymethyl-Methacrylate with High Focusing Control," Applied Surface Science, Vol. 278, pp. 185-189, 2013.
3. Khan Malek, C. G., "Laser Processing for Bio-Microfluidics Applications (Part II)," Analytical and Bioanalytical Chemistry, Vol. 385, No. 8, pp. 1362-1369, 2006.
4. Becker, H. and Locascio, L. E., "Polymer Microfluidic Devices," Talanta, Vol. 56, No. 2, pp. 267-287, 2002.
5. Mathur, A., Roy, S. S., Tweedie, M., Mukhopadhyay, S., Mitra, S., and McLaughlin, J., "Characterisation of PMMA Microfluidic Channels and Devices Fabricated by Hot Embossing and Sealed by Direct Bonding," Current Applied Physics, Vol. 9, No. 6, pp. 1199-1202, 2009.
6. Chang, T. C. and Molian, P. A., "Excimer Pulsed Laser Ablation of Polymers in Air and Liquids for Micromachining Applications," Journal of Manufacturing Processes, Vol. 1, No. 1, pp. 1-17, 1999.
7. Klank, H., Kutter, J. P., and Geschke, O., "CO_2-Laser Micromachining and Back-End Processing for Rapid Production of PMMA-based Microfluidic Systems," Lab on a Chip, Vol. 2, No. 4, pp. 242-246, 2002.
8. Snakenborg, D., Klank, H., and Kutter, J. P., "Microstructure Fabrication with a CO_2 Laser System," Journal of Micromechanics and Microengineering, Vol. 14, No. 2, pp. 182-189, 2004.
9. Berrie, P. G. and Birkett, F. N., "The Drilling and Cutting of Polymethyl Methacrylate (Perspex) by CO_2 Laser," Optics and Lasers in Engineering, Vol. 1, No. 2, pp. 107-129, 1980.
10. Prakash, S., Acherjee, B., Kuar, A. S., and Mitra, S., "An Experimental Investigation on ND: YAG Laser Microchanneling on Polymethyl Methacrylate Submerged in Water," Proceedings of the Institution of Mechanical Engineers, Part B: Journal of Engineering Manufacture, Vol. 227, pp. 508-519, 2013.
11. Prakash, S. and Kumar, S., "Fabrication of Microchannels: A Review," Proceedings of the Institution of Mechanical Engineers, Part B: Journal of Engineering Manufacture, 2014. DOI: 095440541 4535581.
12. Kannatey-Asibu Jr, E., "Principles of Laser Materials Processing," John Wiley & Sons, p. 130, 2008.
13. Wang, Z., Zheng, H., Lim, R., Wang, Z., and Lam, Y., "Improving Surface Smoothness of Laser-Fabricated Microchannels for Microfluidic Application," Journal of Micromechanics and Microengineering, Vol. 21, No. 9, Paper No. 095008, 2011.
14. Yap, Y. C., Guijt, R. M., Dickson, T. C., King, A. E., and Breadmore, M. C., "Stainless Steel Pinholes for Fast Fabrication of High-Performance Microchip Electrophoresis Devices by CO_2 Laser Ablation," Analytical Chemistry, Vol. 85, No. 21, pp. 10051-10056, 2013.
15. Chung, C. K., Tan, T. K., Lin, S. L., Tu, K. Z., and Lai, C. C., "Fabrication of Sub-Spot-Size Microchannel of Microfluidic Chip using CO_2 Laser Processing with Metal-Film Protection," Micro & Nano Letters, Vol. 7, No. 8, pp. 736-739, 2012.
16. Yuan, D. and Das, S., "Experimental and Theoretical Analysis of Direct-Write Laser Micromachining of Polymethyl Methacrylate by CO_2 Laser Ablation," Journal of Applied Physics, Vol. 101, No. 2, Paper No. 024901, 2007.
17. Zakariyah, S. S., Conway, P. P., Hutt, D. A., Wang, K., and Selviah, D. R., "CO_2 Laser Micromachining of Optical Waveguides for Interconnection on Circuit Boards," Optics and Lasers in Engineering, Vol. 50, No. 12, pp. 1752-1756, 2012.
18. Davis, T. A. and Cao, J., "Effect of Laser Pulse Overlap on Machined Depth," Transactions of the North American Manufacturing Research Institution of SME, Vol. 38, pp. 291-298, 2010.
19. Ryan, T. P., "Modern Experimental Design," John Wiley & Sons, pp. 450-452, 2006.